Thermodynamics of Heme Binding to the $HasA_{SM}$ Hemophore: Effect of Mutations at Three Key Residues for Heme Uptake†

Clarisse Deniau,‡,§ Robert Gilli,‡,|| Nadia Izadi-Pruneyre,§ Sylvie Létoffé,⊥ Muriel Delepierre,§ Cécile Wandersman,⊥ Claudette Briand,|| and Anne Lecroisey*,§

Unité de Résonance Magnétique Nucléaire des Biomolécules, CNRS URA 2185, Institut Pasteur, Paris, France, UPRESA, CNRS URA 6032, Marseille, France, and Unité des Membranes Bactériennes, CNRS URA 1300, Institut Pasteur, Paris, France

Received January 13, 2003

ABSTRACT: $HasA_{SM}$ secreted by the Gram-negative bacterium *Serratia marcescens* belongs to the hemophore family. Its role is to take up heme from host heme carriers and to shuttle it to specific receptors. Heme is linked to the $HasA_{SM}$ protein by an unusual axial ligand pair: His32 and Tyr75. The nucleophilic nature of the tyrosine is enhanced by the hydrogen bonding of the tyrosinate to a neighboring histidine in the binding site: His83. We used isothermal titration microcalorimetry to examine the thermodynamics of heme binding to $HasA_{SM}$ and showed that binding is strongly exothermic and enthalpy driven: $\Delta H = -105.4$ kJ·mol^{-1} and $T\Delta S = -44.3$ kJ·mol^{-1}. We used displacement experiments to determine the affinity constant of $HasA_{SM}$ for heme ($K_a = 5.3 \times 10^{10}$ M^{-1}). This is the first time that this has been reported for a hemophore. We also analyzed the thermodynamics of the interaction between heme and a panel of single, double, and triple mutants of the two axial ligands His32 and Tyr75 and of His83 to assess the implication of each of these three residues in heme binding. We demonstrated that, in contrast to His32, His83 is essential for the binding of heme to $HasA_{SM}$, even though it is not directly coordinated to iron, and that the Tyr75/His83 pair plays a key role in the interaction.

Bacteria have developed a number of iron-scavenging mechanisms, depending on the iron sources they might encounter. Heme-containing compounds, which are widespread among vertebrate hosts, are advantageous iron reservoirs for bacterial pathogens. Therefore, several Gram-negative bacteria use a *h*eme *u*ptake *s*ystem involving an extracellular heme-binding protein, HasA, also called hemophore by analogy to the extracellular siderophores (*1*). HasA hemophores are secreted in iron-limiting conditions by an ABC transporter via a carboxy-terminal signal. Their function is to acquire free or hemoprotein-bound heme and to deliver it to a specific outer membrane receptor, HasR (*1*, *2*). HasA hemophores have been found in *Serratia marcescens* (*1*), *Pseudomonas aeruginosa* (*3*), *Pseudomonas fluorescens* (*4*), *Yersinia pestis* (*5*), and *Yersinia enterocolytica* (P. Delepelaire, personal communication). They form an independent family of heme-binding proteins without homology to any other known proteins.

The *S. marcescens* hemophore, $HasA_{SM}$,[1] is a 19 kDa monomer that binds *b* heme with a stoichiometry of 1 (*6*). The crystal structure of the holoprotein shows an original $\alpha + \beta$ fold, with an unusual arrangement of the heme-binding site (*7*). The α helices are all packed on one side of the molecule and the β strands on the other side. Heme is held by two loops at the interface between the α and β parts of the molecule and is highly exposed to solvents. The iron atom is ferric and coordinated to the Nϵ of a histidine residue, His32, on one side and to the Oη of a tyrosine residue, Tyr75, on the other side (Figure 1). Tyrosine, which is weakly nucleophilic, is a rare heme iron ligand. It is only present in catalase (*8*), in *Chlamydomonas* chloroplast hemoglobin (*9*), in nitrite reductase (*10*), and in some proteins in which the axial coordination has been modified by protein engineering (*11*−*14*). Our recent NMR study showed that, in holo-$HasA_{SM}$, the Tyr75 phenolate oxygen is deprotonated and forms a hydrogen bond with the NδH of a neighboring histidine in the binding site, His83 (*15*). Comparison of the affinities of the single, double, and triple alanine mutants of His32, Tyr75, and His83 for heme by absorption spectroscopy suggested that His83 plays an important role in heme ligation and acts an alternative iron ligand in the absence of Tyr75 (*16*). In this work, we used isothermal titration calorimetry (ITC) to determine the affinity of $HasA_{SM}$ and the panel of mutants for heme and to examine the thermodynamics of their heme binding. This is the first time that the affinity of a hemophore for heme has been reported. The

† This work was supported in part by a grant from the Programme de recherche fondamentale en microbiologie et maladies infectieuses parasitaires (Ministère de l'éducation nationale, de la recherche, et de la technologie).

* To whom correspondence should be addressed. Phone: 33.1.40.61.36.67. Fax: 33.1.45.68.89.29. E-mail: alecrois@pasteur.fr.

‡ These authors contributed equally to this work.

§ Unité de Résonance Magnétique Nucléaire des Biomolécules, CNRS URA 2185, Institut Pasteur.

|| UPRESA, CNRS URA 6032.

⊥ Unité des Membranes Bactériennes, CNRS URA 1300, Institut Pasteur.

[1] Abbreviations: ITC, isothermal titration calorimetry; NMR, nuclear magnetic resonance; SDS−PAGE, sodium dodecyl sulfate−polyacrylamide gel electrophoresis; Has, heme acquisition system; $HasA_{SM}$, *Serratia marcescens* hemophore; $HasR_{SM}$, $HasA_{SM}$ receptor.

10.1021/bi030015k CCC: $25.00
Published on Web 08/22/2003

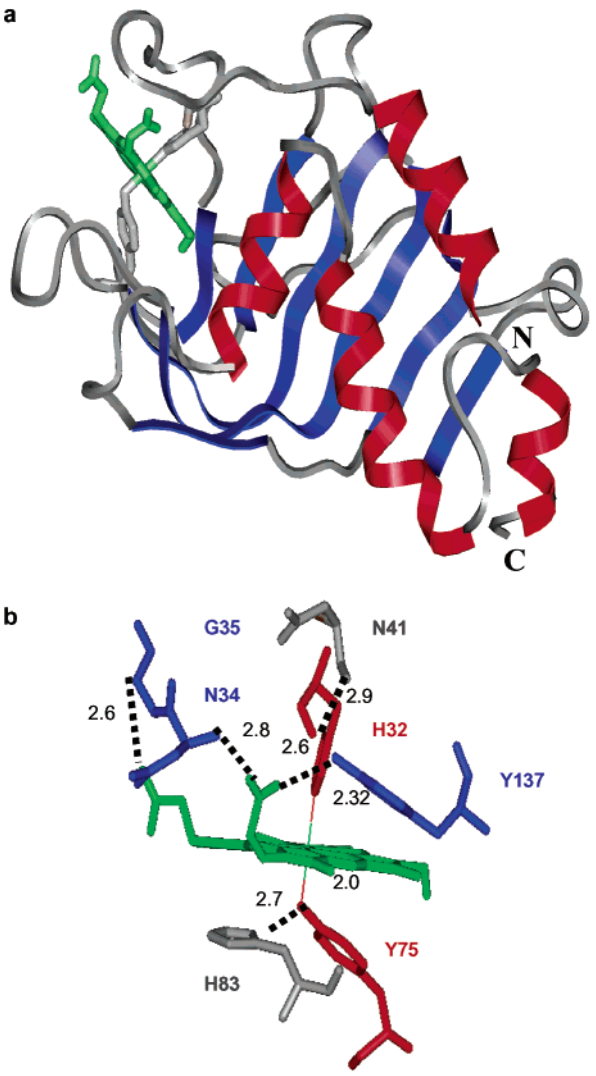

FIGURE 1: Panel a: Backbone structure of holo-HasA_{SM}. A ribbon diagram with helices colored in red and strands in blue is shown. Heme is represented in green. The last 14 residues which gave no X-ray density are not seen on the figure. Panel b: Schematic representation of the heme-binding site of holo-HasA_{SM}. The axial ligands H32 and Y75 are shown in red. Residues linked to axial ligand side chains (N41 and H83) by hydrogen bonds are represented in gray. Residues linked to heme propionate groups (N34, G35, and Y137) by hydrogen bonds are shown in blue. Heme is in green. Hydrogen bonds are represented by dashed lines. Distances are given in angstroms.

heme-binding constants of HasA_{SM} and of some of the mutants were too large to be determined by classical methods; thus we carried out displacement experiments. To evaluate the role of the hydrogen bond between His83 and Tyr75, we replaced His83 with a glutamine residue, the side chain of which could be expected to form a hydrogen bond with the tyrosinate, and measured the energetics of heme binding. Finally, we compared the thermodynamic parameters of the interactions between heme and HasA_{SM} and between heme and the mutants and analyzed the role of the axial ligands and of His83 in heme binding.

MATERIALS AND METHODS

Expression and Purification of the HasA_{SM} Proteins. Single, double, and triple mutated *hasA* genes (H32A, Y75A, H83A, and H83Q) were constructed by in vitro site-directed mutagenesis as described previously (*16*). Wild-type and mutant HasA_{SM} proteins were obtained from the culture supernatants of *Escherichia coli* strain Pop3 (pSYC34PAM) grown at 30 °C in M9 minimal medium and purified as described by Izadi et al. (*6*). All proteins were checked by SDS−PAGE and mass spectrometry. Their concentrations were determined by using the previously determined ϵ_{277} values: 19500 $M^{-1}\cdot cm^{-1}$ for HasA_{SM}, H83A and H83Q; 18500 $M^{-1}\cdot cm^{-1}$ for Y75A, Y75A-H83A, and Y75A-H83Q; 21700 $M^{-1}\cdot cm^{-1}$ for H32A, H32A-H83A, and H32A-H83Q; 19900 $M^{-1}\cdot cm^{-1}$ for H32A-Y75A, H32A-Y75A-H83A, and H32A-Y75A-H83Q (*16*). The natural heme content of HasA_{SM} proteins was determined from the absorbance of their Soret band and was always less than 0.5%. When necessary, the last C-terminal residues of wild-type HasA_{SM} were cleaved by proteolysis with the *S. marcescens* protease PrtSM (*17*).

Preparation of Hemin Solutions. Bovine hemin (Sigma) was dissolved in a minimal volume of 0.1 N NaOH, centrifuged, and diluted to the desired concentration with 50 mM sodium phosphate buffer, pH 7.3. The concentration of the hemin solutions was measured in 0.1 N NaOH using the $\epsilon_{385(0.1N\ NaOH_{aq})}$ value of 58440 $M^{-1}\cdot cm^{-1}$ (*18*). Hemin solutions were freshly prepared just prior to the titrations to prevent heme aggregation.

Isothermal Titration Calorimetry. Titrations were performed at 25 °C using a MicroCal MCS titration calorimeter (MicroCal Inc., Northampton, MA) (*19*). Proteins and hemin were suspended in 50 mM sodium phosphate, pH 7.3. Solutions were thoroughly degassed by stirring under vacuum before use. Due to heme adsorption, the calorimeter cell and the microsyringe used for injections were extensively washed after each experiment.

One of the limitations of common or direct ITC is that it cannot be used to determine high-affinity constants. As the product of the substrate molarity and the K_a value must be between 1 and 1000 (*19*), the low concentration required for high K_a measurements would be associated with too little heat exchange relative to the heat effects generated by dilution and mixing. Thus, we measured affinity constants of up to 10^7-10^8 M^{-1} by direct titration and higher values by displacement ITC (*20*, *21*). Values of about 10^8 M^{-1} could be determined by both methods. Changes in enthalpy (ΔH) and molar stoichiometry (n) were measured by direct titration for all the heme-binding interactions. Changes in free energy (ΔG) and entropy (ΔS) were calculated from the classical relationship $\Delta G = -RT \ln K_a = \Delta H - T\Delta S$, where R is the gas constant and T is the temperature in kelvin. For all titrations, the heat of diluting the ligand was measured by injecting the ligand into the buffer alone or by injecting more ligand into the cell after saturation. The value obtained was subtracted from the heat of reaction to obtain the effective heat of binding.

(A) Direct Titration. Experiments were carried out as follows: a 250 μL microsyringe was used to inject 20−35 volumes of hemin solution (7−10 μL) into the 1.34 mL calorimeter cell containing the protein solution at 3−4 min intervals. The protein concentration was about 10^{-5} M for the wild-type protein and the single mutants, about 5×10^{-5} M for the double mutants except H32A-Y75A (about 10^{-4} M), and up to 4×10^{-4} M for the triple mutants. The hemin concentration was between 5- and 10-fold higher but did not

Table 1: Affinity Constants and Stoichiometries for the Binding of Heme to Wild-Type or Mutated $HasA_{SM}$ in 50 mM Sodium Phosphate Buffer, pH 7.3, at 25 °C[a]

	ITC method	K_a (M^{-1})	n
WT	displacement	$5.3 (\pm 1.6) \times 10^{10}$	1.05 (±0.02)
H32A	displacement	$1.0 (\pm 0.4) \times 10^{10}$	1.11 (±0.09)
Y75A	displacement and direct	$1.3 (\pm 0.3) \times 10^{8}$	1.13 (±0.06)
H83A	displacement and direct	$2.0 (\pm 0.2) \times 10^{8}$	1.03 (±0.11)
H83Q	displacement and direct	$3.4 (\pm 0.2) \times 10^{8}$	1.05 (±0.08)
H32A-Y75A	direct	$5.9 (\pm 1.0) \times 10^{4}$	0.44 (±0.07)
H32A-H83A	direct	$2.3 (\pm 1.2) \times 10^{7}$	0.89 (±0.27)
H32A-H83Q	direct	$2.6 (\pm 1.5) \times 10^{7}$	1.12 (±0.13)
Y75A-H83A	direct	$1.8 (\pm 0.8) \times 10^{6}$	0.87 (±0.12)
Y75A-H83Q	direct	$3.0 (\pm 1.5) \times 10^{6}$	0.97 (±0.03)
H32A-Y75A-H83A	direct	nd	nd
H32A-Y75A-H83Q	direct	nd	nd

[a] n is the stoichiometry for the binding of heme to $HasA_{SM}$ proteins; nd = not determined. K_a and n values are the averages of three to six experiments ± the standard error of the mean.

exceed 5×10^{-4} M except for the triple mutants. Indeed, we did not observe any significant heme aggregation with freshly prepared hemin solutions up to this concentration. The enthalpy of binding (ΔH), affinity constant (K_a), and molar binding stoichiometry (n) were directly obtained from the titration curve fitted using the single-site binding model of Origin software.

(B) Displacement Titration. Heme was displaced from a low-affinity protein to the higher affinity protein of unknown K_a. The H32A-H83Q mutant was used as the low-affinity protein. Heme (10^{-5} to 2×10^{-5} M) was saturated with H32A-H83Q protein (2×10^{-5} to 4.4×10^{-5} M), introduced into the calorimeter cell, and titrated with 20−35 injections of 7−10 μL aliquots of the high-affinity protein (1.2×10^{-4} to 3.3×10^{-4} M). The K_a value was obtained from the titration curve fit using the modified Sigurskjold regression equations from the Origin software (*21*).

RESULTS

Affinity for Heme. (A) Wild-Type $HasA_{SM}$. Previous absorption spectroscopy data indicated that the affinity of wild-type $HasA_{SM}$ for heme was above 10^9 M^{-1}. Direct ITC titration could not determine the affinity of this protein for heme more precisely. The titration curve obtained with the minimal concentration of $HasA_{SM}$ that could be used in the calorimetric cell to obtain a reliable heat emission signal, 10^{-5}M, was indeed too steep at the equivalence point (data not shown). Thus, we used an appropriate low-affinity ligand, the H32A-H83Q mutant, to carry out displacement experiments and to measure the affinity of $HasA_{SM}$ for heme: $K_a = 5.3 (\pm 1.6) \times 10^{10}$ M^{-1} (Table 1). The H32A-H83Q holo mutant was chosen as a heme donor for $HasA_{SM}$ due to its heme-binding parameters, as determined by direct ITC (see below). First, its heme-binding constant value was $2.6 (\pm 1.5) \times 10^7$ M^{-1}; thus we could expect to be able to determine binding constants of between 2 and 5 orders of magnitude larger (i.e., up to 10^{12} M^{-1}). Second, its binding enthalpy ($\Delta H = -29.2$ kJ·mol^{-1}) was sufficiently different from that of $HasA_{SM}$ to obtain a large heat signal following the injection of 7−10 μL. The transition region of the binding isotherm was indeed clearly defined, thus allowing us to measure the $HasA_{SM}$ binding constant accurately. A typical isothermal displacement titration of the H32A-H83Q holo mutant by apo-$HasA_{SM}$ is presented in Figure 2.

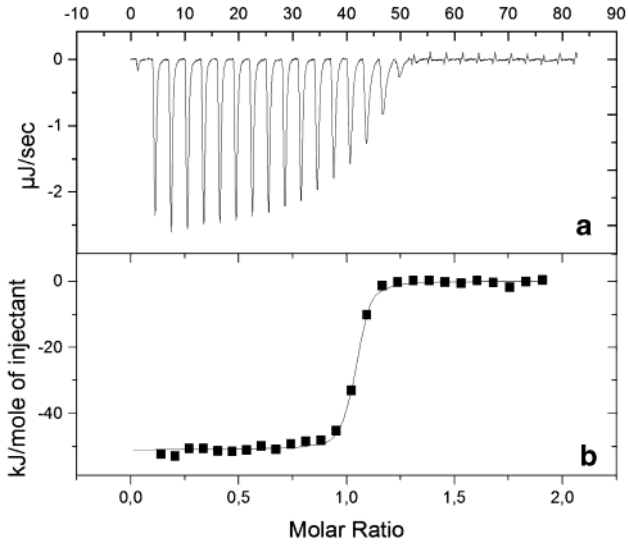

FIGURE 2: Typical isothermal displacement titration calorimetric profile of the binding of heme to $HasA_{SM}$ in 50 mM phosphate, pH 7.3, at 25 °C. Panel a: Heat signal for the titration of holo-H32A-H83Q by apo-$HasA_{SM}$ after subtraction of the heat of dilution of apo-$HasA_{SM}$. Twenty-eight injections of 7 μL of apo-$HasA_{SM}$ (1.67×10^{-4} M) into the reaction cell containing 1.34 mL of H32A-H83Q (4.28×10^{-5} M), 65% saturated with heme, were performed at 3 min intervals. Panel b: Binding isotherm derived from (a).

We previously showed that the hemophore secreted by *S. marcescens* lacks the last 11 residues of its C-terminal secretion signal and is thus shorter than the recombinant *E. coli* $HasA_{SM}$ protein (*17*). As demonstrated by NMR, this region is highly flexible and unstructurated in $HasA_{SM}$. We checked that the affinity for heme of both proteins was identical by measuring the affinity of the short form of $HasA_{SM}$ obtained by cleavage of its C-terminal extremity by the *S. marcescens* protease PrtSm, as described by Izadi-Pruneyre et al. (*17*): $K_a = 5.2 (\pm 1.5) \times 10^{10}$ M^{-1}.

(B) Mutant Proteins. The affinity constants of the single, double, and triple mutants are given in Table 1. The decrease or loss of affinity observed for all the mutants does not correspond to major structural rearrangements of the proteins compared to in the wild-type $HasA_{SM}$ since the circular dichroism spectra of the proteins are all similar (data not presented). However, the double mutation H32A-Y75A and the two triple mutations have an obvious destabilizing effect since the proteins aggregate at a concentration of 10^{-4}−10^{-5} M. Preliminary NMR studies of the other mutant proteins in the concentration range between 0.2 and 2×10^{-3} M do not display any spectral change with time at 30 °C.

(i) Single Mutants. The affinity of the H32A mutant was too large to be measured by direct ITC titration. Therefore, it was determined by the displacement method, using the same low-affinity ligand and heme donor as for $HasA_{SM}$, the H32A-H83Q holo mutant. The affinities of the Y75A, H83A, and H83Q mutants were determined by both direct and displacement ITC titration.

Axial ligands His32 and Tyr75: The mutation of the two iron axial ligands did not produce a similar effect on heme binding. The mutation of His32 resulted in a 5-fold decrease in affinity, whereas the mutation of Tyr75 resulted in a 400-

Table 2: Thermodynamic Parameters for the Binding of Wild-Type or Mutated $HasA_{SM}$ to Heme in 50 mM Sodium Phosphate Buffer, pH 7.3, at 25 °C[a]

	ΔH (kJ·mol^{-1})	ΔG (kJ·mol^{-1})	$T\Delta S$ (kJ·mol^{-1})	n	coupling ΔG
WT	−105.4 (±3.8)	−61.1 (±0.8)	−44.3 (±3.9)	1.05 (±0.02)	
H32A	−72.2 (±3.3)	−57.1 (±1.1)	−15.1 (±3.5)	1.11 (±0.09)	
Y75A	−74.4 (±6.9)	−46.4 (±1.6)	−28.0 (±7.1)	1.13 (±0.06)	
H83A	−62.2 (±4.2)	−47.3 (±0.3)	−14.9 (±4.2)	1.03 (±0.11)	
H83Q	−89.1 (±6.6)	−48.7 (±2.0)	−40.4 (±6.9)	1.05 (±0.08)	
H32A-Y75A	−25.8 (±3.3)	−27.2 (±0.5)	−1.4 (±3.3)	0.44 (±0.07)	15.2 (±2.2)
H32A-H83A	−41.1 (±7.4)	−42.0 (±1.3)	−0.9 (±7.5)	0.89 (±0.27)	1.3 (±1.9)
H32A-H83Q	−29.2 (±5.6)	−42.3 (±2.4)	13.1 (±6.1)	1.12 (±0.13)	2.4 (±3.4)
Y75A-H83A	−35.0 (±1.3)	−35.7 (±1.0)	0.6 (±1.7)	0.87 (±0.12)	−3.1 (±2.1)
Y75A-H83Q	−54.0 (±11.7)	−36.9 (±1.3)	−17.0 (±12)	0.97 (±0.03)	−2.9 (±3.0)

[a] ΔH, ΔG, and $T\Delta S$ values are the average of three to six experiments. ΔH and ΔG values are given ± the standard deviation (SD) of the mean. The errors on $T\Delta S$ values were calculated as $[SD^2(\Delta H) + SD^2(\Delta G)]^{1/2}$. ΔG_c is the coupling free energy between residues H32, Y75, and H83. The errors on ΔG_c values were calculated as $[\sum SD^2(\Delta G)]^{1/2}$.

fold decrease. The length of the two axial bonds determined from the X-ray structure of holo-$HasA_{SM}$ was 2 Å for the Tyr75Oη−Fe bond and 2.32 Å for the His32Nϵ2−Fe bond, suggesting that Tyr75 was indeed a stronger ligand than His32. However, such a large difference between the affinities of the H32A and Y75A mutants for heme was unexpected as, in Y75A, the axial residue Tyr75 may be replaced by the His83 residue whereas, in H32A, a water molecule probably coordinates to iron instead of His32. Indeed, we previously showed that His83 might become an alternative iron ligand in the absence of both natural axial ligands His32 and Tyr75 (*16*), and we cannot exclude the possibility that this also happens when only Tyr75 is mutated.

The replacement of His83 by alanine or glutamine produced a 260-fold and a 150-fold decrease in affinity, respectively. Thus, the loss of affinity induced by the mutation of His83 is much greater than that induced by the mutation of His32, even though His32 is an axial ligand and His83 is not, and suggests that His83 plays a crucial role in heme binding. We previously demonstrated that His83 remains protonated up to pH = 9.7 in holo-$HasA_{SM}$ and that it is the proton donor in the Tyr75−His83 hydrogen bond whereas Tyr75 is the proton acceptor. The Tyr75−His83 hydrogen bond thus stabilizes the Tyr75Oη−Fe ligation by enhancing the nucleophilic character of the tyrosinate. In addition, it probably helps to maintain the tyrosine ring in the correct orientation so that it can tightly bind iron. Thus, the differences in the strengths of the Tyr75−Fe and His32−Fe bonds are the result of the strong interaction between the tyrosinate and His83. The fact that the affinity is reduced 150-fold in H83Q and 260-fold in H83A suggests that the glutamine side chain is involved in a hydrogen bond with Tyr75 and that this bond stabilizes the ligation of the tyrosinate to iron. This bond would, however, be weaker than the His83−Tyr75 hydrogen bond in wild-type $HasA_{SM}$.

(ii) Double and Triple Mutants. The affinities of the double and triple mutants were determined by direct titration. The mutation of both His32 and His83 produced a 10^3-fold decrease in affinity and the mutation of both Tyr75 and His83 a 10^4-fold decrease. There was no significant difference between the effects of the H83A and H83Q mutations. The mutations of both His32 and Tyr75 had a much larger effect on the affinity, with a 10^6-fold decrease, but the affinity remained significant. Conversely, no heat exchange could be detected for either of the triple mutants (H32A-Y75A-H83A and H32A-Y75A-H83Q). Only the heat dilution signal of hemin was observed at protein concentrations of up to 4×10^{-4} M (higher concentrations could not be used because they caused protein aggregation). These data confirm our previous results, showing that His83 allows the heme−protein interaction to occur in the absence of both natural axial ligands (*16*).

Heme-Binding Stoichiometry. The fit of the titration curves gave molar binding stoichiometries close to 1 for all of the proteins except H32A-Y75A. Thus, no significant heme aggregation occurred in our experimental conditions. Moreover, for some of the mutants, titrations of the protein (in the microsyringe) with hemin (in the cell) gave similar results to the titration of hemin with the protein (data not shown). The loss of stoichiometry observed for H32A-Y75A (n = 0.44) suggests that the protein was partially aggregated at the concentrations required for ITC experiments (between 7.4×10^{-5} and 1.3×10^{-4} M). This hypothesis is reinforced by the result of a preliminary differential scanning calorimetry study on the thermal stability of $HasA_{SM}$ proteins, which showed that the H32A-Y75A mutant tends to aggregate (unpublished results).

Thermodynamics of the Interactions. The thermodynamic parameters of the heme $HasA_{SM}$ protein interactions are summarized in Table 2.

(A) Wild-Type $HasA_{SM}$. The binding of heme to wild-type $HasA_{SM}$ resulted in a large favorable negative change in enthalpy [ΔH = −105.4 (±3.8) kJ·mol^{-1}] and in an unfavorable negative change [$T\Delta S$ = −44.3 (±3.9) kJ·mol^{-1}]. Binding is thus strongly enthalpy-driven, which is consistent with a polar process of interaction. In holo-$HasA_{SM}$, heme is highly exposed to solvent (186 Å^2) and maintained in a stable orientation by various polar interactions (*7*, *22*). It is linked to the protein by three hydrogen bonds involving its propionate groups and by the two semipolar bonds between its ferric iron and the two axial ligands. Furthermore, a network of hydrogen bonds between the core of the protein and residues of the binding pocket helps in its anchorage. These polar interactions thus make a major contribution to heme binding despite the hydrophobicity of the binding pocket residues (*7*) and of the protoporphyrin.

The negative ΔS value shows that the loss of degrees of freedom, associated with a decrease in entropy (unfavorable change), has a larger effect than the gain in hydrophobic contacts due to the release of water molecules associated with an increase in entropy (favorable change).

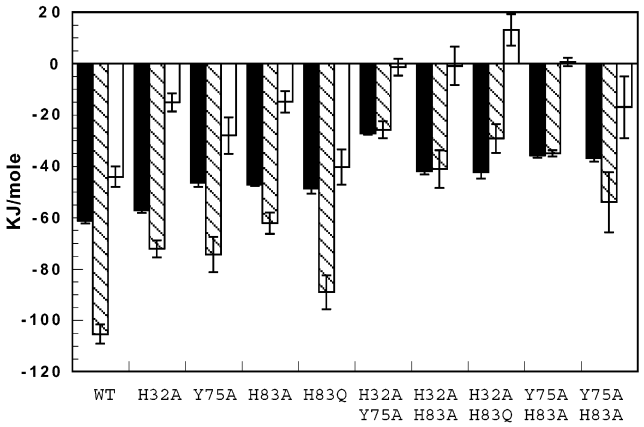

FIGURE 3: Thermodynamic profiles for the binding of heme with the wild-type or mutated $HasA_{SM}$ in 50 mM sodium phosphate buffer, pH 7.3, at 25 °C. ΔG is shown in black, ΔH in stripes, and $T\Delta S$ in white. The error bars represent the errors on the values given in Table 2.

(B) Mutant Proteins. The mutations did not qualitatively affect the forces that drive the heme binding as all of the mutants showed enthalpy-driven thermodynamic interaction profiles such as $HasA_{SM}$ (Figure 3). However, the binding enthalpies of the mutants were always less favorable than for the wild-type protein: $\Delta\Delta H = (\Delta H_{mutant} - \Delta H_{WT}) > 0$. This increase in binding enthalpy was partially compensated by an increase in binding entropy: $\Delta\Delta S = (\Delta S_{mutant} - \Delta S_{WT}) > 0$, inducing an overall increase in free energy and thus a loss of affinity: $\Delta\Delta G = (\Delta G_{mutant} - \Delta G_{WT}) > 0$. These results are consistent with a loss and/or a weakening of the axial bonds in the mutant proteins. The loss or the weakening of strong polar interactions generates an unfavorable enthalpy change. However, since the anchorage of heme is less tight, there is a subsequent gain of degrees of freedom which induces a favorable increase in binding entropy. It is likely that modifications of the heme coordination in the different mutants cause small changes in its position within the binding site in comparison with the wild-type protein. These differences in heme position as well as small conformational changes in the loop backbone and/or residue side chains may also contribute to an increase in hydrophobic contacts and in binding entropy.

(i) Single Mutants. H32A: The His32 mutation led to the loss of the His32−Fe axial bond and of the hydrogen bond between the imidazole and residue Asn41 (His32Nδ−Asn41O bond). It also resulted in a large increase in binding entropy, $\Delta\Delta H = 33.2$ kJ·mol^{-1}, but only a modest change in free energy, $\Delta\Delta G = 4$ kJ·mol^{-1}, due to a large entropy compensation, $\Delta(T\Delta S) = 29.2$ kJ·mol^{-1}. Although a water molecule probably coordinates to iron instead of His32 in H32A, heme is less constrained than in $HasA_{SM}$ and binding entropy is less unfavorable.

Y75A: The mutation of Tyr75 led to the loss of the Y75−Fe axial bond and of the hydrogen bond involving the tyrosinate and His83 (Tyr75Oη−His83Nδ). $\Delta\Delta H$ (31 kJ·mol^{-1}) was similar to that observed for the H32A mutant, but entropy compensation was lower, $\Delta(T\Delta S)$ (16.3 kJ·mol^{-1}), and thus $\Delta\Delta G$ was higher (14.7 kJ·mol^{-1}). We have previously shown that His83 acts as an alternative iron ligand when both axial ligands (His32 and Tyr75) are mutated and that His83 probably replaces Tyr75 and coordinates to iron in the single Y75A mutant. However, in this case, the His83−Fe bond is weak as the affinity of Y75A for heme is 400-fold lower than that of $HasA_{SM}$. In wild-type holo-$HasA_{SM}$, the His83 imidazole ring is parallel to the heme plane, and the Nδ and Nϵ nitrogens are located about 4 and 5 Å from the iron atom, respectively. In hemoproteins with a histidine as an axial ligand, the imidazole ring is totally or almost perpendicular to the heme plane, and the His−Fe bond measures less than 2.5 Å in length. His83 is therefore not in the correct position to become an axial ligand, and its coordination to iron requires some minor conformational changes, the contribution of which to the heme-binding thermodynamic parameters is impossible to evaluate.

H83A and H83Q: Both mutations induced similar changes in free energy ($\Delta\Delta G = 13.8$ and 12.4 kJ·mol^{-1}, respectively); however, the contributions of enthalpy and entropy to the decreases of affinity differed. The H83A mutation was associated with a large increase in enthalpy ($\Delta\Delta H = 43.2$ kJ·mol^{-1}), consistent with the loss of the tight hydrogen bond between His83NδH and Tyr75Oη, thus decreasing the strength of the Tyr75−Fe axial bond. In the case of the H83Q mutation, enthalpy was increased only by 16.3 kJ·mol^{-1}. The difference between the binding enthalpies of H83A and H83Q supports the hypothesis that a hydrogen bond was formed between the Gln83 side chain and Tyr75O in H83Q. The binding entropy changes observed for H83A and H83Q are also consistent with the hypothesis that residues 75 and 83 interact with each other: the gain in compensating entropy was high for H83A [$\Delta(T\Delta S) = 29.4$ kJ·mol^{-1}] and modest for H83Q [$\Delta(T\Delta S) = 3.9$ kJ·mol^{-1}]. Hydrogen bonding of Tyr75 to Gln83 would indeed stabilize heme within the binding pocket and reduce the degrees of freedom of H83Q with regard to H83A. The length of the glutamine side chain as compared to that of alanine may also reduce the degrees of freedom.

(ii) Double Mutants. Like the single mutants and wild-type $HasA_{SM}$, the double mutants showed enthalpy-driven thermodynamic interaction profiles of heme binding. Binding enthalpies were, however, less favorable. The increase in binding enthalpy ($\Delta\Delta H = \Delta H_{mutant} - \Delta H_{WT}$) was larger than the corresponding increase in binding free energy ($\Delta\Delta G = \Delta G_{mutant} - \Delta G_{WT}$) due to a large compensating gain in binding entropy.

We evaluated the degree of cooperation between the pairs of residues upon binding by the double mutant cycle method (*23*−*25*) with the equation:

$$\Delta G_c = \Delta G_{XY} + \Delta G_{X\rightarrow A,Y\rightarrow A} - (\Delta G_{X\rightarrow A} + \Delta G_{Y\rightarrow A})$$

where ΔG_c is the coupling free energy, ΔG_{XY} is the free energy of the wild-type protein, $\Delta G_{X\rightarrow A}$ and $\Delta G_{Y\rightarrow A}$ are the free energies of the single mutants X → A and Y → A, and $\Delta G_{X\rightarrow A,Y\rightarrow A}$ is the free energy of the double mutant. If the effects of the two mutations are independent or additive, ΔG_c should be zero. If the effects of the two mutations are related or nonadditive, the change in energy for the double mutants should be different from the sum of the change in energy for the two single mutants and $\Delta G_c \neq 0$. If $\Delta G_c > 0$, the coupling is unfavorable, and the presence of the first residue hinders the binding of the second. If $\Delta G_c < 0$, the coupling is favorable. Nonzero coupling free energies may be associated with either a direct steric contact between the residues or a short-range steric interaction involving triangulation through a mediating molecule (*26*, *27*).

H32A-Y75A: The H32A-Y75A double mutation led to the loss of both the natural His32−Fe and Tyr75−Fe axial bonds. It induced a drastic increase in binding free energy ($\Delta\Delta G = 33.9$ kJ·mol^{-1}) and binding enthalpy ($\Delta\Delta H = 79.6$ kJ·mol^{-1}) despite a large entropy compensation [$\Delta(T\Delta S) = 45.7$ kJ·mol^{-1}]. In the mutant, iron is probably coordinated to a water molecule on one side, in place of His32, and to His83 on the other side, in place of Tyr75. As described above, His83 is not in the correct position to act as an axial ligand, and conformational changes have to occur to allow its coordination to iron. Unfortunately, it is impossible to evaluate the contribution of these changes to each of the thermodynamic parameters.

The coupling free energy between residues His32 and Tyr75 was positive and thus unfavorable (15.2 kJ·mol^{-1}), which means that the binding of His32 to heme iron hinders the fixation of Tyr75 and vice versa. This result is consistent with the fact that the side chains of His32 and Tyr75 are oriented such that the formation of one optimized axial bond (length and inclination relative to heme plane) prevents the second one from being optimized.

H32A-H83A and H32A-H83Q: The free binding energies of H32A-H83A and H32A-H83Q were similar. However, the binding enthalpy was less favorable for H32A-H83Q ($\Delta H = -29.2$ kJ·mol^{-1}) than for H32A-H83A ($\Delta H = -41.1$ kJ·mol^{-1}), and subsequently binding entropy was more favorable ($T\Delta S = 13.1$ kJ·mol^{-1} and $T\Delta S = -0.9$ kJ·mol^{-1}, respectively). This was not expected. The glutamine side chain is longer than the alanine side chain, and Glu83 probably forms a hydrogen bond with Tyr75. Thus, H32A-H83Q presents less degrees of freedom than H32A-H83A. This suggests that the heme-binding pocket of H32A-H83A is reorganized to allow Tyr75 to bind iron more efficiently. For example, the tyrosine ring might move such that it is perpendicular to the heme plane.

The coupling free energy between residues His32 and His83 is weakly positive and thus unfavorable (1.3 and 2.4 kJ·mol^{-1} for H32A-H83A and H32A-H83Q, respectively). Although the two residues are not in direct contact, they communicate through the iron atom and Tyr75. As expected, coupling between residues His32 and His83 is less unfavorable than coupling between residues His32 and Tyr75 as His83 is not directly involved in the ligation of iron.

Y75A-H83A and Y75A-H83Q: The free binding energies of Y75A-H83A and Y75A-H83Q were weaker than those observed for the His32/His83 mutation. This confirms that the Tyr75/His83 pair plays a major role in heme binding. Both mutants had comparable free binding energies, whereas Y75A-H83A had a much lower binding enthalpy and therefore a larger entropy compensation [$\Delta\Delta H = 70.4$ kJ·mol^{-1} and $T(\Delta\Delta S) = 44.9$ kJ·mol^{-1} versus $\Delta\Delta H = 51.4$ kJ·mol^{-1} and $T(\Delta\Delta S) = 27.3$ kJ·mol^{-1}]. This result may reflect the larger steric hindrance of the glutamine side chain and/or the hydrogen bonding of Gln83 with residues encompassed in the heme-binding pocket.

The coupling free energies between residues Y75 and H83 were small and favorable, which show that these two residues interact directly. This result is consistent with the fact that His83 favors the binding of Tyr75 to iron by enhancing the nucleophilic nature of the tyrosinate and by holding the tyrosine ring in the correct orientation through hydrogen bonds.

DISCUSSION

It is difficult to measure the affinity of heme-binding proteins for heme because the ligand aggregates easily. Therefore, there are often discrepancies between the reported heme-binding constant obtained using different measurement methods, especially for high-affinity proteins. Absorption spectroscopy can be used for affinities of up to 10^7-10^8 M^{-1}, depending on the intensity of the Soret band. Higher affinities cannot be measured directly. They are usually calculated from the ratio of the association and dissociation rate constants or estimated following the transfer of heme from another heme-binding protein with a lower heme-binding constant to the protein of interest. Robinson et al. used direct ITC to determine the heme-binding constant of cytochrome b_{562} ($K_a = 1.1 \times 10^8$ M^{-1}) (*28*). Here, we used displacement ITC for the first time to measure the heme-binding constant of a hemoprotein, the $HasA_{SM}$ hemophore. The K_a value determined, 5.3×10^{10} M^{-1}, is among the highest reported for a heme-binding protein. Only myoglobin, with a K_a of around 10^{14} M^{-1}, has a higher affinity for heme than $HasA_{SM}$ (*29*), which is consistent with our data showing that the myoglobin does not deliver its heme to $HasA_{SM}$ (S. Létoffé, unpublished results). The exact affinities of each chain of the hemoglobin tetramer for heme are not known, but the fact that $HasA_{SM}$ can take heme from hemoglobin suggests that the hemophore has a higher affinity than hemoglobin (*30*). Hemopexin has a similar affinity for heme as $HasA_{SM}$: $K_a = 6.8 \times 10^{10}$ M^{-1} (*31*). The affinities for heme of other heme-binding proteins such as human serum albumin (*32*), bovine serum albumin (*33*), and high- and low-density lipoproteins (*31*) are several orders of magnitude lower than that of $HasA_{SM}$.

All the single and double $HasA_{SM}$ mutants except H32A-Y75A still had a high affinity for heme with K_a values between 10^{10} M^{-1} and 3×10^6 M^{-1}. Single mutations of His32 and Tyr75 had a unusually low effect on heme binding, especially that of His32, which only induced a 5-fold decrease in affinity. The mutation of Tyr75 induced a 400-fold decrease. However, as His83 becomes an axial ligand when Tyr75 is mutated, it is more accurate to estimate the contribution of Tyr75 to heme binding from the affinity of the Y75A-H83A double mutant for heme. The Fe−Tyr75 bond accounts for a factor of 10^4 regarding the equilibrium association constant, which is close to that estimated for axial coordination in metmyoglobin (*29*). Both axial ligands make a very uneven contribution to heme binding. Such a disparity has also been observed between the two axial histidines of cytochrome b_5, and it has been shown that the histidine with the highest affinity is part of a very flexible loop (*34*). Dynamic studies of $HasA_{SM}$ are now in progress to determine whether the loop encompassing Tyr75 exhibits larger fluctuations than the loop encompassing His32.

The crucial role of His83 in the binding of heme to $HasA_{SM}$ relies on the stabilization of the Tyr75Oη−Fe bond and on its ability to become an alternative ligand. The tyrosinate ion is also stabilized by hydrogen bonds in other hemoproteins. In nitrite reductase, the phenolate oxygen is hydrogen bonded to a water molecule that is itself hydrogen bonded to two histidines (*10*, *35*). In catalase, the tyrosine oxygen shares a proton with the positively charged side chains from an arginine (*8*, *36*). In the alkaline ferric form

of *Chlamydomonas* chloroplast hemoglobin, the side chain of a lysine helps to stabilize the Fe−O bond by inhibiting the protonation of the tyrosinate. It is noteworthy that, like His83 in $HasA_{SM}$, this lysine may become an axial ligand and coordinate to the heme when the tyrosine is mutated to an alanine (*9*).

A large number of hydrophobic interactions stabilizing heme in the binding pocket is usual for hemoproteins due to the hydrophobic nature of protoporphyrin. In globins, hydrophobic contacts between the protoporphyrin and apolar residues of the binding pocket are prevalent. In myoglobin, they account for about half of the free energy, the other half being shared between the formation of the axial bond and specific electrostatic interactions with residues in the heme cavity (*29*). In $HasA_{SM}$, the formation of hydrophobic contacts is not the major factor of the heme−protein association. Axial bonds and electrostatic interactions are predominant and heme binding is strongly enthalpy-driven. The binding of heme to apocytochrome b_{562} shows similar features: favorable changes in binding enthalpy ($\Delta H = -71.1$ kJ·mol^{-1}) and unfavorable changes in binding entropy ($T\Delta S = -23.7$ kJ·mol^{-1}) (*28*). However, the contribution of the hydrophobic interactions is greater than for the hemophore. In cytochrome b_5, hydrophobic interactions are not predominant during heme binding (*37*). Analysis of the thermodynamic parameters of the wild-type $HasA_{SM}$ and of the mutant proteins demonstrated that the Tyr75−Fe axial bond and the Tyr75−His83 hydrogen bond are the most important interactions between heme and the protein. We previously showed that His83 controls the protonation state of Tyr75Oη. Moreover, unlike His32, the Tyr75/His83 pair is conserved in the eight other known hemophores. Taken together, these data suggest that the Tyr75/His83 pair is the key factor involved in the interaction between heme and the hemophore HasA.

REFERENCES

1. Letoffe, S., Ghigo, J. M., and Wandersman, C. (1994) *Proc. Natl. Acad. Sci. U.S.A. 91*, 9876−9880.
2. Ghigo, J. M., Létoffé, S., and Wandersman, C. (1997) *J. Bacteriol. 179*, 3572−3679.
3. Létoffé, S., Redeker, V., and Wandersman, C. (1998) *Mol. Microbiol. 28*, 1223−1234.
4. Létoffé, S., Omori, K., and Wandersman, C. (2000) *J. Bacteriol. 182*, 4401−4405.
5. Rossi, M. S., Fetherston, J. D., Létoffé, S., Carniel, E., Perry, R. D., and Ghigo, J. M. (2001) *Infect. Immun. 69*, 6707−6717.
6. Izadi, N., Henry, Y., Haladjian, J., Goldberg, M. E., Wandersman, C., Delepierre, M., and Lecroisey, A. (1997) *Biochemistry 36*, 7050−7057.
7. Arnoux, P., Haser, R., Izadi, N., Lecroisey, A., Delepierre, M., Wandersman, C., and Czjzek, M. (1999) *Nat. Struct. Biol. 6*, 516−520.
8. Fita, I., and Rossmann, M. G. (1985) *J. Mol. Biol. 185*, 21−37.
9. Das, T. K., Couture, M., Lee, H. C., Peisach, J., Rousseau, D. L., Wittenberg, B. A., Wittenberg, J. B., and Guertin, M. (1999) *Biochemistry 38*, 15360−15368.
10. Baker, S. C., Saunders, N. F., Willis, A. C., Ferguson, S. J., Hajdu, J., and Fulop, V. (1997) *J. Mol. Biol. 269*, 440−455.
11. Goodwin, D., Rowlinson, S., and Marnett, L. (2000) *Biochemistry 39*, 5422−5432.
12. Liu, Y., Moenne-Loccoz, P., Hildebrand, D. P., Wilks, A., Loehr, T. M., Mauk, A. G., and Ortiz de Montellano, P. R. (1999) *Biochemistry 38*, 3733−3743.
13. Maurus, R., Bogumil, R., Luo, Y., Tang, H. L., Smith, M., Mauk, A. G., and Brayer, G. D. (1994) *J. Biol. Chem. 269*, 12606−12610.
14. Nagai, M., Yoneyama, Y., and Kitagawa, T. (1989) *Biochemistry 28*, 2418−2422.
15. Wolff, N., Deniau, C., Létoffé, S., Simenel, C., Kumar, V., Stojiljkovic, I., Wandersman, C., Delepierre, M., and Lecroisey, A. (2002) *Protein Sci. 11*, 757−765.
16. Létoffé, S., Deniau, C., Wolff, N., Dassa, E., Delepelaire, P., Lecroisey, A., and Wandersman, C. (2001) *Mol. Microbiol. 41*, 439−450.
17. Izadi-Pruneyre, N., Wolff, N., Redeker, V., Wandersman, C., Delepierre, M., and Lecroisey, A. (1999) *Eur. J. Biochem. 261*, 562−568.
18. Dawson, R., Elliott, D., Elliott, W., and Jones, K. (1986) *Data for biochemical research*, Oxford University Press, Oxford.
19. Wiseman, T., Williston, S., Brandts, J. F., and Lin, L. N. (1989) *Anal. Biochem. 179*, 131−137.
20. Sigurskjold, B. W., Berland, C. R., and Svensson, B. (1994) *Biochemistry 33*, 10191−10199.
21. Sigurskjold, B. W. (2000) *Anal. Biochem. 277*, 260−266.
22. Fersht, A. R., Matouschek, A., and Serrano, L. (1992) *J. Mol. Biol. 224*, 771−782.
23. Carter, P. J., Winter, G., Wilkinson, A. J., and Fersht, A. R. (1984) *Cell 38*, 835−840.
24. Horovitz, A., Serrano, L., Avron, B., Bycroft, M., and Fersht, A. R. (1990) *J. Mol. Biol. 216*, 1031−1044.
25. Fersht, A. R., Matouschek, A., and Serrano, L. (1992) *J. Mol. Biol. 226*, 771−782.
26. Li Cata, V. J., and Ackers, G. K. (1995) *Biochemistry 34*, 3133−3139.
27. Bradshaw J. M., and Waksman G. (1999) *Biochemistry 38*, 5147−5154.
28. Robinson, C. R., Liu, Y., Thomson, J. A., Sturtevant, J. M., and Sligar, S. G. (1997) *Biochemistry 36*, 16141−16146.
29. Hargrove, M. S., and Olson, J. S. (1996) *Biochemistry 35*, 11310−11318
30. Létoffé, S., Faribado, N., Goldberg, M., and Wandersmann, C. (1999) *Mol. Microbiol. 33*, 546−555.
31. Miller, Y. I., and Shaklai, N. (1999) *Biochim. Biophys. Acta 1454*, 153−164.
32. Gattoni, M., Boffi, A., Sarti, P., and Chiancone, E. (1996) *J. Biol. Chem. 271*, 10130−10136.
33. Benesh, R. (1994) *Methods in Enzymology*, Vol. 231, Academic Press, New York.
34. Ihara, M., Takahashi, S., Ishimori, K., and Morishima, I. (2000) *Biochemistry 39*, 5961−5970.
35. Williams, P., Fulop, V., Garman, E., Saunders, N., Ferguson, S., and Hajdu, J. (1997) *Nature 389*, 406−412.
36. Gouet, P., Jouve, H., and Dideberg, O. (1995) *J. Mol. Biol. 249*, 933−954.
37. Falzone, C., Wang, Y., Vu, C., Scott, N., Bhattacharya, S., and Lecomte, J. (2001) *Biochemistry 40*, 4879−4891.

BI030015K